Taylor & Francis
Taylor & Francis Group

ORIGINAL RESEARCH

🔓 OPEN ACCESS   Check for updates

Studying TIGIT activity against tumors through the generation of knockout mice

Ahmed Rishiq[a], Reem Bsoul[b], Ophir Pick[a], and Ofer Mandelboim[a]

[a]The Concern Foundation Laboratories at the Lautenberg Center for Immunology and Cancer Research, Institute for Medical Research Israel Canada (IMRIC), Hebrew University-Hadassah Medical School, Jerusalem, Israel; [b]The Institute of Dental Sciences, The Hebrew University-Hadassah School of Dental Medicine, Jerusalem, Israel

ABSTRACT
The use of antibodies to block inhibitory receptors, primarily anti-PD1 and CTLA4 (known as checkpoint therapy) revolutionized cancer treatment. However, despite these successes, the majority of cancer patients do not respond to the checkpoint treatment, emphasizing the need for development of additional therapies, which are based on other inhibitory receptors. Human TIGIT is an inhibitory receptor expressed by Natural Killer (NK) and T cells and is mainly known to interact with PVR, Nectin-2, Nectin-3, and Nectin-4. Whether mouse TIGIT interacts with all of these ligands is still unclear. Additionally, the in vivo function of TIGIT against tumors is not completely understood. Here, we demonstrate that mouse TIGIT interacts with and is inhibited by mPVR only. Using CRISPR-Cas9 technology, we generated TIGIT-deficient mice and demonstrated that NK cell cytotoxicity and degranulation against two tumor types were lower in WT mice when compared to the TIGIT KO mice. Moreover, in vivo tumor progression was slower in TIGIT KO than in WT mice. Taken together, our data established that mTIGIT has only one ligand, PVR, and that in the absence of TIGIT tumors are killed better both in vitro and in vivo.

Introduction

Maintaining a balance between inhibitory and activating receptors is crucial for immune homeostasis as well as for the protection of the organism from autoimmune diseases and immunopathology during infection[1]. In recent years, it was also recognized that blocking inhibitory receptors using antibodies (known as checkpoint blockade immunotherapy) is an effective treatment for cancer patients[2]. The two most efficient drugs in this category are antibodies directed against CTLA-4 and PD-1 named, for example, ipilimumab and nivolumab, respectively[3]. Other inhibitory receptors, against which blocking antibodies are currently at various stages of development, are Lag-3, Tim-3, and TIGIT[4].

TIGIT (T-cell Immunoreceptor with Ig and ITIM domains) is an inhibitory receptor expressed on both activated T and NK cells[5]. It has a type I transmembrane domain containing an external immunoglobulin variable-set (IgV) domain and an intracellular domain with one ITT-like motif and one ITIM motif, which transmit the inhibitory signal[5,6]. Murine TIGIT (mTIGIT) shares 58% homology with human TIGIT, while the cytoplasmic tail is identical in human and mice[7].

Previous research has established that human TIGIT interacts with PVR (also known as CD155 or Necl-5), Nectin-2 (CD1112 or PVRL2), Nectin-3 (CD113 or PVRL3), and Nectin-4 (CD113 or PVRL4)[8]. The bacterial Fap2 protein, which is expressed by Fusobacterium nucleatum and mediates adhesion to various bacteria and tumors, was also found to interact with human TIGIT but not with mouse TIGIT[9]. Fungal ligands belonging to the Als (Agglutinin-Like

Sequences) protein family were reported to bind both human and mouse TIGIT[10]. Collectively, the interaction between TIGIT and its various ligands inhibits immune cell activities.

Whether mouse TIGIT recognize the same ligands recognized by human TIGIT is still unclear. Stanietsky et al. found that the murine B12 cell line that expresses mPVR was recognized by a mouse TIGIT fusion protein (mTIGIT-Ig), and further demonstrated that mTIGIT inhibits NK-cell cytotoxicity[7], suggesting that it will be beneficial to block TIGIT interaction with its ligands for better recognition and elimination of tumors. Indeed, anti-TIGIT monoclonal antibodies are employed in clinical trials, either as a single agent or in conjunction with other inhibitory receptors, such as anti-PDL1 or anti-PD1 antibodies[11]. Tiragolumab, Vibostolimab, and Etigilimab are three humanized anti-TIGIT mAbs that have recently been tested in clinical studies. They were used either alone, or in combination with atezolizumab (anti-PDL1), pembrolizumab, or nivolumab. The anti-TIGIT antibodies were used in clinical trials of solid tumors including metastatic non-small cell lung cancer (NCSLC). Patients showed promising but not very potent results[12–14]. Thus, it is quite important to determine which tumors will be susceptible to anti-TIGIT therapy using knockout mice and also to precisely determine the identity of the mouse cellular ligands for TIGIT. Here, we generated a TIGIT knockout mouse (TIGIT KO) using the CRISPR Cas9 genetic engineering technology to test tumor development in the absence of TIGIT, and determined that murine TIGIT interacts only with PVR.

Materials and methods

Generation of TIGIT knockout (TIGIT KO) mice

TIGIT KO mice were generated by CRISPR-Cas9 knockout and HDR editing of C57BL/6JOlaHsd mouse genome with the help of the Genetic Engineered Mouse Models (GEMM) National Israeli Facility at the Hebrew University of Jerusalem. A single guide RNA (sgRNA), recognizing TIGIT gene 5′-TTCAGTCTTCAGTGATCGGG-3'at the genomic region followed by 5'-TGG-3' PAM sequence, was designed and purchased from Integrated DNA Technologies (IDT). The designed murine TIGIT gRNA recruited the Cas9 DNA endonuclease, which introduced a double-strand break resulting in a 41-bases deletion mutation. TIGIT sgRNA then annealed with constant Tracer RNA and was then mixed with Cas9 enzyme, and subsequently introduced directly to the zygote by electroporation. Finally, the electroporated zygote was transferred to the embryo-recipient pseudo-pregnant mouse. To test whether the mice have the desired mutation, an ear punch was acquired and transferred into 100 µL of DNA extraction buffer (100 µL of 1 M NaOH and 6 µL of 0.5 M EDTA in 10 mL ultra-pure water) and then boiled at 100°C for 10 min. The primers used for genotyping were: mTIGIT KO F-5‘CCAGAGACTCACGTGTGCTT-3’ and mTIGIT KO R-5‘GGTGGTGTTTCCTATGTGAGAG-3’. PCR products were detected on a 1.5% agarose gel. PCR products obtained were: mTIGIT wild type (WT): one band of 424 bp, mTIGIT knockout (mTIGIT KO): one band of 383 bp, while mTIGIT heterozygous (mTIGIT Het) contained two bands; 424 bp and 383 bp. DNA products of the PCR reaction were then extracted from the gel, purified, and then confirmed by Sanger sequencing (HyLabs).

PCR reaction* was performed using the following protocol.

Step	Temperature	Time
1- Denaturation	98C°	30 seconds
2- Denaturation	98 C°	10 seconds
3- Annealing	63 C°	30 seconds
4- Elongation	72 C°	15 seconds
5- Steps (2–4) 30 cycles		
6-Elongation	72 C°	10 minutes

*Using Phusion High-Fidelity DNA Polymerase (F530L, Thermoscientific).

Cell culture

B16F10 and MC38 cells were maintained in Dulbecco's Modified Eagle's Medium (DMEM) and 721.221 cells were maintained in Roswell Park Memorial Institute culture medium (RPMI), both supplemented with 10% fetal calf serum, 1% Pen/Strep, 1% L-glutamine, 1% MEM Eagle, and 1% sodium pyruvate. The generation of 721.221 cells expressing mNectin2 and mPVR was previously described[7]. All cells were incubated in a humidified incubator with 5% CO2 at 37°C. The IL-2 activation medium is composed of DMEM and F12 combination medium supplemented with 10% human serum, 1% Pen/Strep, 1% L-glutamine, 1% MEM Eagle, and 1% sodium pyruvate and 400 U/mL IL-2 (PeproTech).

Knockout of mPVR with CRISPR Cas9 system in tumor cells

B16F10 and MC38 tumor cell lines were stably infected to express Cas9 using the recombinant LentiCas9-Blast plasmid (Addgene, 52962) as previously described[15]. mPVR single oligonucleotides (sgRNAs) F:5'CACCGGGCCAAGAGATTCGTCCAGG'3 and R:5'AAACCCTGGACGAATCTCTTGGCCC3' were designed following the instructions described by CrispRGold (https://crispr gold.mdc-berlin.de/). The designed sgRNAs were annealed and then sub-cloned into BsmBI digested lentiGuide-Puro (Addgene, 52963), and insertion was confirmed by Sanger sequencing.

Fusion protein, antibodies, and flow cytometry

Murine TIGIT-Ig fusion protein was produced as previously described[7,16]. Variable concentrations of mTIGIT-Ig 0.5, 1, 2.5 and 5 µg were used in FACS assays. Binding was detected by a secondary antibody (Allophycocyanin anti-human IgG, Jackson), at a dilution of 1:200, after incubation for 30 min on ice.

PE-conjugated anti-mouse CD335 (NKp46)/Ncr1 and allophycocyanin-conjugated anti-mouse TIGIT (Vstm3) (BioLegend) were employed to identify mouse NK cells and mTIGIT. PE-conjugated anti-mouse CD279 (PD-1) and anti-mouse CEACAM1 and allophycocyanin-conjugated anti-mouse CD274 (PDL-1), I-A/I-E (MHCII), and CD223 (LAG3) (BioLegend) were used to identify PD-1,CEACAM1, PDL-1, MHCII, and LAG3. To detect mouse PVR and Nectins, purified anti-mouse CD155/PVR, Nectin-1,2,3, and 4 antibodies (R&D Systems) were used. All staining was performed with 0.2 µg antibody per 100,000 cells. Binding was detected by a secondary antibody (Alexa Flour 647 anti-mouse IgG, Jackson), at a dilution of 1:200, after incubation for 30 min on ice. All steps were performed as previously described[16]. All results were analyzed using the FCS Express 6 software.

Calcein AM release cytotoxicity assay

B16F10 and MC38 were harvested and centrifuged at 1600 rpm for 5 min. The cells were then washed using RPMI serum-free medium, and then centrifuged at 1600 rpm for 5 min. 10 µL (50 µg) of Calcein AM (C1430, Thermoscientific) was added per 2×10^6 cells in 2 mL of RPMI serum-free medium, mixed thoroughly, and then incubated for 30 min at 37°C. Labeled cells were then washed twice with RPMI serum-free medium and re-suspended in 2 mL of RPMI with 10% serum and counted. Murine splenocytes were produced from freshly harvested spleens of WT and TIGIT KO mice as previously described[10]. Isolated mice splenocytes were either activated with IL-2, or not activated, and then incubated with the calcein AM-labeled target cells (10,000 cells/well were seeded in 96 U-shaped plates) in an effector to target (E: T) ratio of 5:1 for 3 h at 37°C. 100 µL of supernatant was harvested and transferred into black flat bottom 96-well plates. The calcein spontaneous release was calculated using B16F10 and MC38 cells alone (without NK cells). Maximal calcein release is tumor cells treated with TritonX100 (9.8 mL RPMI with serum and 200 µL of TritonX-100). Fluorescence from each sample was

measured using SPARK® multimode microplate reader (Excitation 485 ± 20 nm and Emission 535 ± 20 nm). The relative calcein release was calculated as relative calcein release % = (Sample-calcein spontaneous release/maximal calcein release-calcein spontaneous release)*100.

Degranulation assay

For murine NK cell CD107a degranulation assay, isolated mice splenocytes were first activated with IL-2 and then incubated with the target cells in an effector-to-target (E:T) ratio of 1:2 in the presence of an anti-mouse CD107a antibody and PE-conjugated anti-mouse CD335 (NKp46)/Ncr1 (BioLegend) for 2 h at 37°C. Through Ncr1^{+} and mCD107a^{+} double labeling, flow cytometry was used to assess the mCD107a levels on the NK cells.

Mice tumor experiments

2×10^6 of B16F10 and MC38 tumor cells, in 100 μL PBS, were inoculated subcutaneously into the right flank region of the WT and TIGIT KO mice. B16F10 in TIGIT KO mice was assessed for 21 days, with samples taken on day 16. Tumor size and mice body weights were measured every 2–3 days using the Spurtar Vernier caliper and the tumor volume in mm[3] was calculated by the modified ellipsoidal formula: $V = Length X Width X Width X 0.5$[17]. When the tumor size reached the humane endpoint (1.5 cm), mice were euthanized as specified for each tumor type. For antibody blocking experiments, WT and TIGIT-KO mice were injected intraperitoneally with or without anti-TIGIT mAb used for TIGIT blockade (anti-mouse TIGIT clone 1G9, BioXCell, 100 μg/mouse). Injections were once every 48 h starting one day prior to B16F10 and MC38 tumor injection. Following animal sacrifice, tumors were harvested and weighed.

Statistics

All statistical analysis was performed and graphs were plotted using GraphPad Prism 8 (GraphPad Software). Statistical significance and differences were determined using unpaired Student's t-test and p value was considered significant at p < 0.05. For multiple comparisons, one-way analysis of variance (ANOVA) with post hoc Tukey's multiple comparisons test was used.

Results

Generating of TIGIT knockout mice

TIGIT knockout (TIGIT KO) mice were generated using a CRISPR-Cas9 knockout genome editing system. TIGIT encompasses three major domains: an extracellular IgV domain, a transmembrane domain and cytoplasmic domain containing an immunoreceptor tyrosine-based inhibitory motif (ITIM) and an immunoglobulin tyrosine tail (ITT)-like motif (Figure 1a)[5,6]. A murine TIGIT single guide RNA (sgRNA) was designed to target the IgV domain (Figure 1a). To confirm deletion, we constructed primer pairs with the

forward primer on intron1 and the reverse primer on intron 2 (since the deletion is located on exon 2) (Figure 1b). We observed a double stranded break in the TIGIT gene at the extracellular domain region, which resulted in a 41-nucleotide deletion and a STOP codon.

We next bred the TIGIT heterozygote mice and obtained WT mice, heterozygotes, and TIGIT KO mice. Accordingly, the PCR product for the WT mice was 424 bp, TIGIT KO 383 bp, and Heterozygous (Het) 424 bp and 383 bp (Figure 1c). The deletion mutation was confirmed by Sanger sequencing of PCR products (Figure 1b,c).

To further demonstrate that TIGIT was indeed knocked out, we isolated splenocytes from WT and TIGIT KO and double stained them with anti-TIGIT and anti-mouse Ncr1 (to detect mostly NK cells Figure 1d), anti-mouse CD3 (to detect T cells Figure 1e), anti-mouse CD4 (to detect T helper cells Figure 1f), and anti-mouse CD8 (To detect CTL Figure 1g). Staining was performed either at day 0 or 2 days after incubation of the splenocytes in IL-2. As can be seen, only a small proportion of NK cells express TIGIT at resting conditions (day 0, Figure 1d) and the entire NK cell population becomes TIGIT positive following IL-2 stimulation (Figure 1d). A small proportion of T cells express TIGIT, and TIGIT expression is increased following IL-2 stimulation (Figure 1e). It seems as if CD4^{+} T cells are those expressing TIGIT under resting conditions because TIGIT expression was detected on CD4^{+} T cells, but not CD8^{+} T cells (Figure 1f,g respectively). TIGIT expression was upregulated on both CD4^{+} and CD8^{+} T cells following IL-2 stimulation. Importantly, no TIGIT expression was detected on splenocytes obtained from TIGIT KO mice, both before and after stimulation (Figure 1d-g). Thus, we are able to generate TIGIT KO mice.

Mouse PVR is the only TIGIT ligand expressed by B16F10 and MC38

In humans, Nectin-2, Nectin-3, Nectin-4, and PVR were demonstrated to be TIGIT ligands, unlike Nectin-1[5,16,18]. We therefore tested the expression of these ligands on mouse B16F10 and MC38 tumor cell lines. No expression of Nectin-1 or Nectin-4 was detected, while both cells lines expressed Nectin-2, Nectin-3, and PVR (Figure 2a). We also stained the tumor cell lines for the expression of ligands for LAG3 (MHC class II), PD-1 (PDL-1) and TIM3 (CEACAM1) (Figure 2b). As can be seen, the tumor cell lines do not express MHC class II, both express PD-L1 and only B16F10 expresses CEACAM1.

To test whether mouse Nectin-2, Nectin-3, and PVR can interact with TIGIT, we generated 721.221 transfectants expressing mNectin-2 and mPVR and validated expression using FACS (Figure 2c). We next used a mouse TIGIT-Ig fusion protein that we have generated previously[7], in which the extracellular portion of mouse TIGIT is fused to human IgG1. Various concentrations of murine TIGIT-Ig fusion protein (0.5, 1, 2.5, and 5 μg) were used to stain the mNectin-2 and mPVR 721.221 transfectants, with parental 721.221 cells serving as control (Figure 2e).
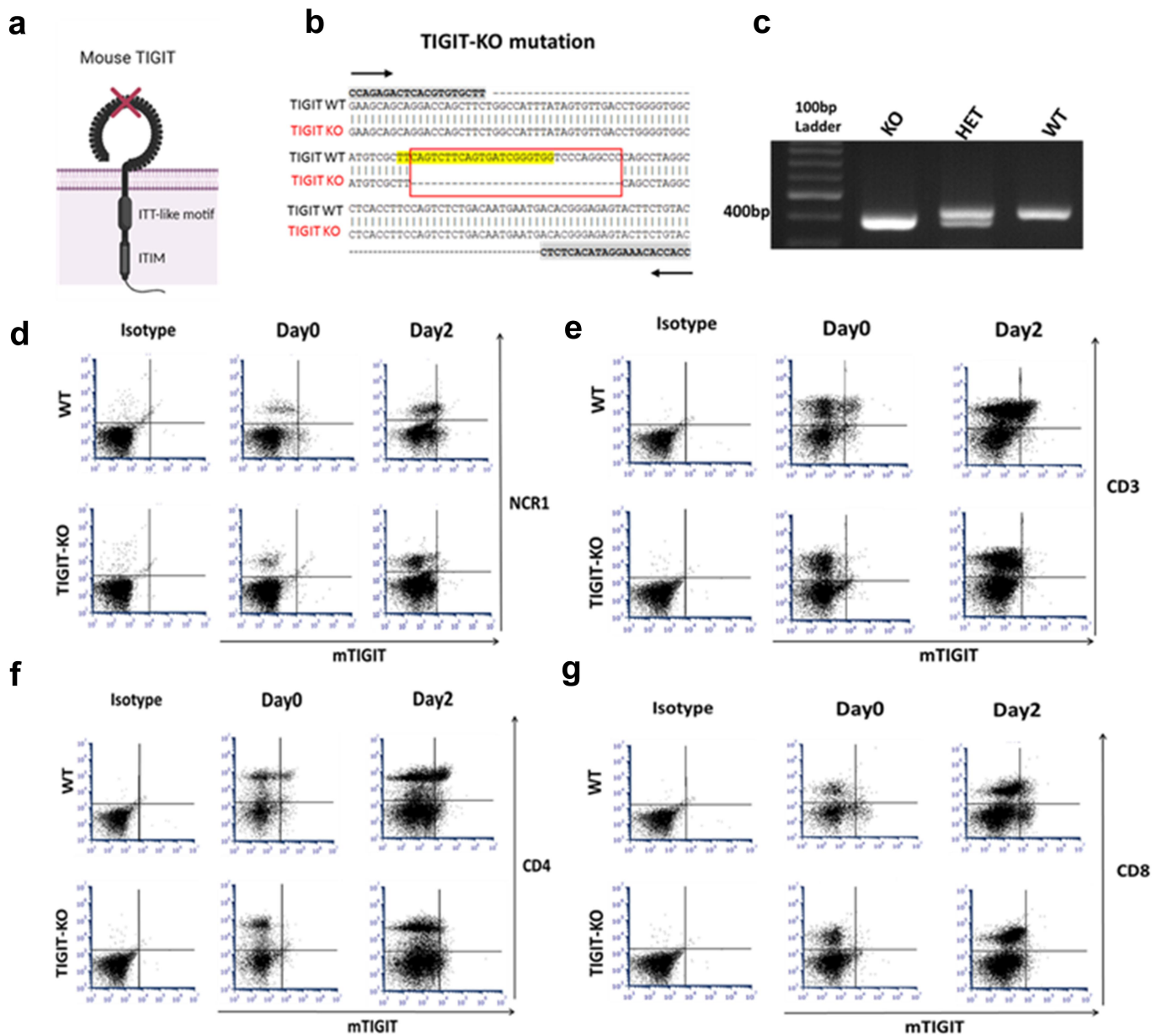
Figure 1. TIGIT KO mouse generation using CRISPR.Cas9 technology. A. a schematic representation of the CRISPR/Cas9 genome editing system of mouse TIGIT. TIGIT contains three domains: An extracellular IgV domain where the mutation is located (indicated as red X), a transmembrane domain and cytoplasmic domain containing an immunoreceptor tyrosine-based inhibitory motif (ITIM) and an immunoglobulin tyrosine tail (ITT)-like motif B. TIGIT CRISPR guide RNA (gRNA) sequence (highlighted nucleotides in yellow) designed to target the TIGIT gene within the mouse genome. A 41 bp deletion mutation (Red framed box) was detected using the designed forward and reverse primers (highlighted nucleotides in gray, marked with black arrows). c. PCR products of TIGIT-KO 383 bp, Heterozygous (Het) 424 bp and 383 bp, and WT 424 bp. D. Flow cytometry plots of isolated splenocytes obtained from WT and TIGIT KO mice and stained with anti-mouse isotype control or with anti-TIGIT together with anti-mouse Ncr1 (D), anti-mouse CD3 (E), anti-mouse CD4 (F), and anti-mouse CD8 (G), at day 0 or 2 following incubation with IL-2.

While efficient binding of TIGIT-Ig was observed to mPVR, no binding was detected to the parental 721.221 cells or to 721.221 cells expressing Nectin-2 (Figure 2e). We next knocked out mPVR in B16F10 and MC38 cell lines using CRISPR-Cas9 genome editing technology. Subsequently, an anti-mouse PVR antibody was used to verify PVR knockout using FACS (Figure 2e). Next, we stained the mPVR KO tumors with mTIGIT-Ig. Importantly, in the absence of PVR (Figure 2e), no mTIGIT-Ig binding was observed (Figure 2f). These results indicate that PVR is the only TIGIT ligand expressed by B16F10 and MC38 cell lines.

mTIGIT suppresses cytotoxicity and degranulation

We next tested whether mouse TIGIT inhibits NK cell cytotoxicity against B16F10 and MC38 cell lines. Because expression of TIGIT is low on resting NK cells (Figure 1d) we isolated splenocytes from WT and TIGIT KO mice and incubated them with IL-2 for 3 days. Subsequently, the activated splenocytes were co-cultured either alone or with calcein-labeled B16F10 and MC38 tumor cell lines for 3 h. Then, the calcein release was measured and the cytotoxic percentages were calculated.

As can be seen, increased cytotoxicity against both cell lines was observed using splenocytes obtained from the TIGIT KO mice when compared to WT mice (Figure 3a).
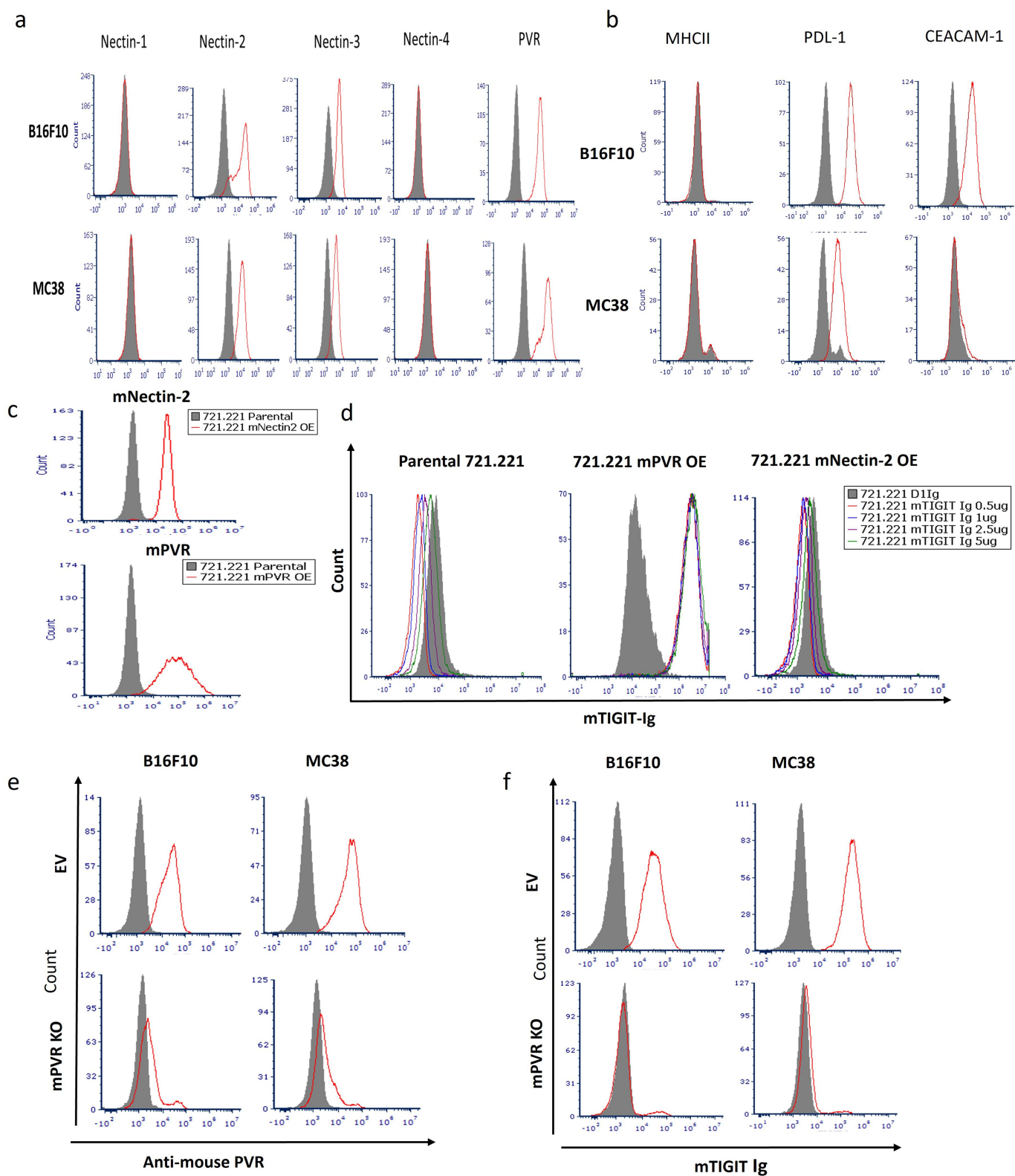
Figure 2. Expression of Nectins family members by B16F10 and MC38 tumor cell lines. A. Flow cytometry analysis of mice Nectin-1, Nectin-2, Nectin-3, Nectin-4, and PVR and B. MHC II, PDL-1 and CEACAM1 (indicated above the histograms), expressed on B16F10 and MC38 tumor cell lines. The gray-filled histograms are the control staining. Red histograms are the staining with the antibodies against each Nectin member (A) and MHC II, PDL-1, and CEACAM1 (B). C. Flow cytometry staining of parental 721.221 (gray filled histogram) and 721.221 cells overexpressing mNectin-2 (red histogram, upper panel) or mPVR (red histogram, lower panel). D. Various mTIGIT-Ig concentrations (indicated in the figure) were used to stain the parental 721.221 cells (left histogram), 721.221 mPVR OE cells (middle histogram), and 721.221 mNectin-2 OE cells (right histogram). The gray histogram is the staining of the cells with a controlled antibody. E. mPVR was knocked out in B16F10 and MC38 using CRISPR.Cas9, and then the parental cells expressing an empty vector (EV, upper) and the knockout cells (mPVR KO, lower) were stained with anti-mouse PVR. F. Flow cytometric staining of the EV expressing cells (upper) or the KO (lower) B16F10 and MC38 cells with mTIGIT-Ig. The gray-filled histograms are the control staining. Red line histogram represents specific staining as indicated.
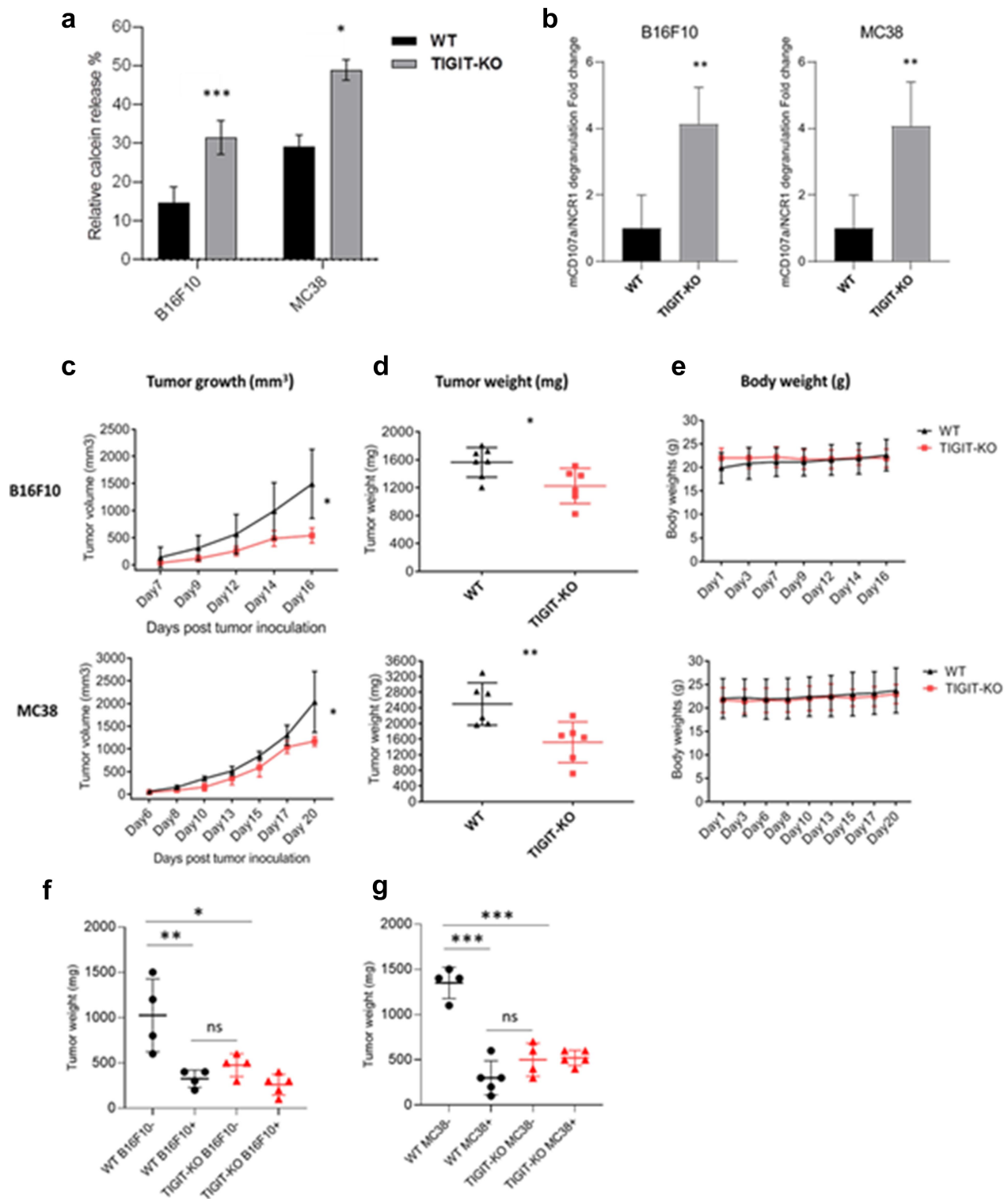
Figure 3. TIGIT knockout increases NK cytotoxicity and suppresses in vivo tumor development. A. Shown is the mean percentage lysis of B16F10 and MC38 tumor cells co-cultured with either WT or TIGIT-KO splenocytes in E: T ratio of 5:1. Incubation was performed for 3 h (n=5). The calcein spontaneous release was calculated using B16F10 and MC38 cells alone (without NK cells). Maximal calcein release is the tumor cells treated with TritonX100. The relative calcein release was calculated as indicated in the materials and method section. B. Fold change of mCD107a expression on NK cells (detected by anti-Ncr1) of WT and TIGIT KO splenocytes (n=6), incubated with B16F10 and MC38 tumors in E: T ratio of 1:2 for 2 h. C. 2×10^6 of B16F10 (upper) and MC38 (lower) tumor cells were injected s.c. into TIGIT-KO and WT mice (n=5–8 per group) and tumor size was followed (D). When tumors reached size of 1.5 cm (considered as an ethical end point), mice were scarified, tumors excised and weighted (mg) (D). E. Body weights of the mice along the experiment. Tumor weight (mg) of WT and TIGIT KO mice (n=4–5 per group) either treated as in (C) or TIGIT was i.p blockade with anti-mouse TIGIT antibody on days −1, 3, 6, 9 and 12 after B16F10 (F) and MC38 (G) tumor implantation. Values are shown as mean ± SD. *P < 0.05, and **$P \leq 0.01$, and *** $P \leq 0.001$.

To further corroborate these results, we also determined NK cell degranulation in the presence of B16F10 and MC38 cell lines. Tumor cells were incubated with activated splenocytes in the presence of anti-mouse Ncr1 and anti-mouse CD107a for 2 h and expression of CD107a on the surface of the Ncr1-positive NK cells was determined. As expected, there was a significant increase (~4-fold change difference) in degranulation between activated TIGIT KO and WT NK cells against both tumor cell lines (Figure 3b). Taken together, these results indicate that TIGIT suppresses NK cell function.

Enhanced *in vivo anti-tumor immunity of TIGIT KO mice*

To investigate whether TIGIT KO mice will have an increased anti-tumor immunity, TIGIT KO and WT mice were inoculated subcutaneously with melanoma (B16F10) and colon adenocarcinoma (MC38) cell lines in the right upper flank. Tumor size (length and width) and mice body weights were measured every 2–3 days. When tumor reached 1.5 cm (considered as the ethical end-point), mice were sacrificed and tumors harvested. Tumor volume was calculated by the modified ellipsoidal formula as indicated in the materials and methods section. In comparison to WT controls, we observed that in the absence of TIGIT tumor development was significantly inhibited (Figure 3c, B16F10 upper, MC38, lower Figure 3c). Concurrently, tumor weight was lower in TIGIT KO mice relative to WT controls in both tumor models (Figure 3d). However, no differences were observed in body weights between WT and TIGIT KO mice throughout the experiment (Figure 3e). To address whether the anti-tumor activity of TIGIT KO will be similar to blocking with anti-TIGIT mAb, B16F10, and MC38 tumors were injected into WT and TIGIT-KO mice with or without anti-TIGIT mAb used for TIGIT blockade. We found that there was no difference between the tumor weight of WT and TIGIT-KO B16F10 (Figure 3f) and MC38 (Figure 3c) tumor-bearing mice injected with anti-TIGIT mAb. Collectively, these results indicate that TIGIT impedes immune cell cytotoxicity *in vivo*, and this effect is apparently mediated by direct interaction with PVR.

No difference in co-inhibitory receptors LAG3 and PD-1 expression between tumor-bearing WT and TIGIT KO mice

We next wanted to examine the expression of other inhibitory receptors: LAG3 and PD-1 in control and tumor-bearing WT and TIGIT KO mice. We first examined TIGIT expression on NK and T cells isolated from splenocytes from WT and TIGIT KO in control and in mice bearing B16F10 and MC38 tumors and observed no TIGIT expression in the KO mice (Figure 4a). Similarly, expression of LAG3 and PD-1 was evaluated. Interestingly, no differences were observed in PD-1 (Figure 4b) and LAG3 (Figure 4c) expression between WT and TIGIT KO in NK and T cells derived from the spleen of control and tumor-bearing mice. Subsequently, we further examined TIGIT, LAG3, and PD-1 expression on NK and T cells isolated from tumor-infiltrating lymphocytes (TILs) from WT and TIGIT KO tumor-bearing mice. While we observed that TIGIT expression was practically not detected on NCR1, CD4^{+}, and CD8^{+} T cells that infiltrated melanoma and colorectal tumors (Figure 5a), no differences were observed in PD-1 (Figure 5b) and LAG3 (Figure 5c) expression on TILs. Our findings therefore suggest that the TIGIT ablation can inhibit tumor progression independently of PD-1 and LAG3.

Discussion

Several studies in human and mice have shown that TIGIT is an important inhibitory checkpoint receptor expressed by NK and T cells[1]. Previous reports indicated that mTIGIT can interact with mPVR, but whether mTIGIT could also recognize mouse Nectin-2 and Nectin-3 still remained largely unknown. Recently, our lab showed that Nectin-4 binds human TIGIT but not its murine orthologue[16].

Here we investigated whether mouse TIGIT interacts with mouse tumor cell lines B16F10 and MC38. Interestingly, we observed that the interaction of mouse TIGIT with its ligands is different than human TIGIT. Using 721.221 cell transfectants expressing Nectin-2, we observed no interaction between mTIGIT and mNectin-2. Further support of this data was the fact that when PVR was knocked out in tumor cell lines B16F10 and MC38 that also express Nectin-2 and Nectin-3, no mTIGIT-Ig binding was detected.

One explanation for the lack of binding of mNectin-2 to mTIGIT-Ig despite the former's expression is that mNectin-2 expression on B16F10 and MC38 tumor cell lines is relatively low compared to mPVR as the staining show. Accordingly, we checked mNectin-2/mTIGIT Ig interaction in mNectin-2 transfectant 721.221 cells and observed no binding, indicating that mTIGIT does not interact with mNectin2. In addition, our lab has previously found that mTIGIT Ig does not crossreact with hPVR, whereas hTIGIT Ig binds mPVR. Moreover, hDNAM-1 and hTIGIT recognize hNectin-2 but both failed to interact with mNectin-2[7]. These data probably indicate that mNectin-2 might lose the site binding to TIGIT and DNAM-1.

TIGIT has previously been associated with T cell exhaustion in colorectal cancer[19], liver cancer[20], acute myelogenous leukemia (AML)[21], and melanoma patients[22]. While the expression of the co-stimulatory receptor DNAM-1 showed no difference between TIGIT^{+} and TIGIT^{−} CD8^{+} T cells, targeting TIGIT together with PD-1 reversed T cell exhaustion and showed promising and effective anti-tumor immunity[19]. Recently, dual blockade of PD1 and TIGIT exhibited full restoration of DNAM-1 signaling and ameliorated anti-tumor CD8^{+} T cell response in non-small lung cancer (NSLC) patients[23]. However, despite TIGIT/PD-1 dual blockade restoring DNAM-1 signaling, they are independently required to regulate DNAM-1[23]. Here, we show that the expression of both PD1 and LAG3 is not altered following TIGIT KO, neither in splenocytes nor in TILs isolated from the tumors, indicating that the effect seen in the KO mice is TIGIT-dependent. Indeed, when we compared the effect of anti-TIGIT blocking antibody to that of the TIGIT KO mice, no differences were observed.

Using surface plasmon resonance (SPR) and staining with Ig-fusion proteins, our lab demonstrated that PVR has higher affinity to mTIGIT when compared to DNAM-1 (a co-stimulatory receptor)[7]. How the absence of mTIGIT will affect
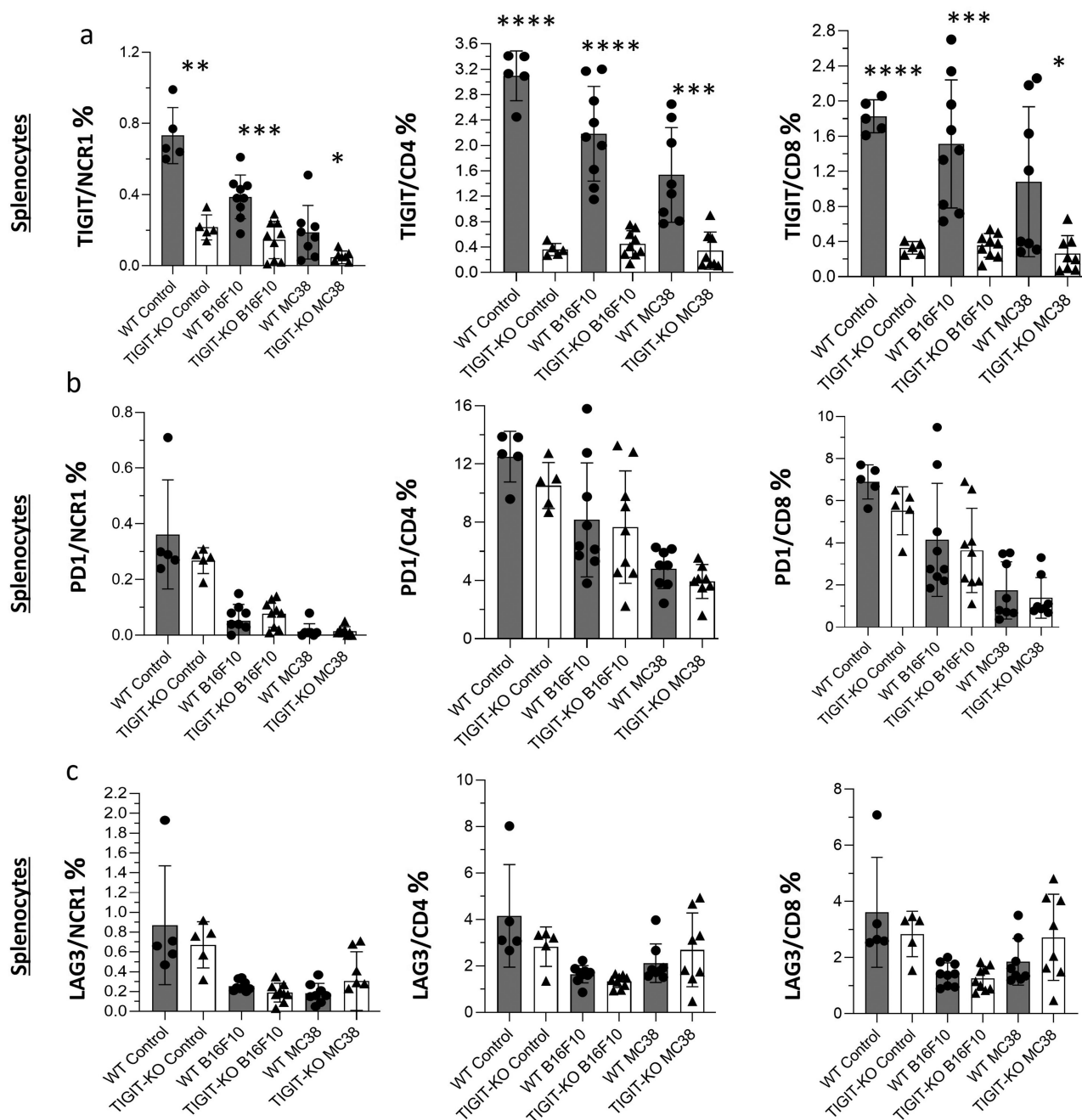
Figure 4. PD-1 and LAG3 are not involved in tumor suppression in splenocytes of TIGIT KO mice. Bar graphs representing the flow cytometry analysis of isolated splenocytes obtained from control WT and TIGIT KO mice or from B16F10 and MC38 bearing mice stained with anti-TIGIT (A) or anti-PD-1 (B) or anti-LAG3 (C) together with anti-mouse Ncr1, anti-mouse CD4, and anti-mouse CD8 antibodies. Values are shown as mean ± SD. *$P < 0.05$, and **$P \leq 0.01$, *** $P \leq 0.001$ and **** $P \leq 0.0001$.

DNAM-1 and mPVR interaction and the consequent function is currently unclear. In one study, PVR deletion in the melanoma cell-line MEL04 increased IFNg release but had no effect when TIGIT was blocked[24]. Additionally, the authors of this work showed that PVR-KO B16F10 cells grew slower than WT tumors when tested *in vivo* with the immune checkpoint inhibitors (ICIs) anti-PD1 and anti-CLTA-4 mAbs[24]. Another study reported that PVR-KO mice displayed reduced B16F10 and MC38 tumor development and metastasis due to DNAM-1 upregulation and improved effector function of CD8+ T-cells and NK cells[25]. A previous study showed that cytotoxic

T lymphocyte (CTL) and NK cells of DNAM-1-deficient mice were considerably less cytotoxic against tumors than WT mice[26]. Here, we demonstrate that TIGIT-KO splenocytes had stronger cytotoxicity and degranulation than WT splenocytes against B16F10 and MC38 cell lines. Consistent with this, *in vivo* TIGIT-KO mice had slower tumor growth and tumor weight relative to WT mice.

A previous report[27] contradicts our findings in which TIGIT knockout was shown to have no impact on murine tumor growth in B16F10 and MC38 tumor models. However, many papers support our results in that Tigit knockout mice
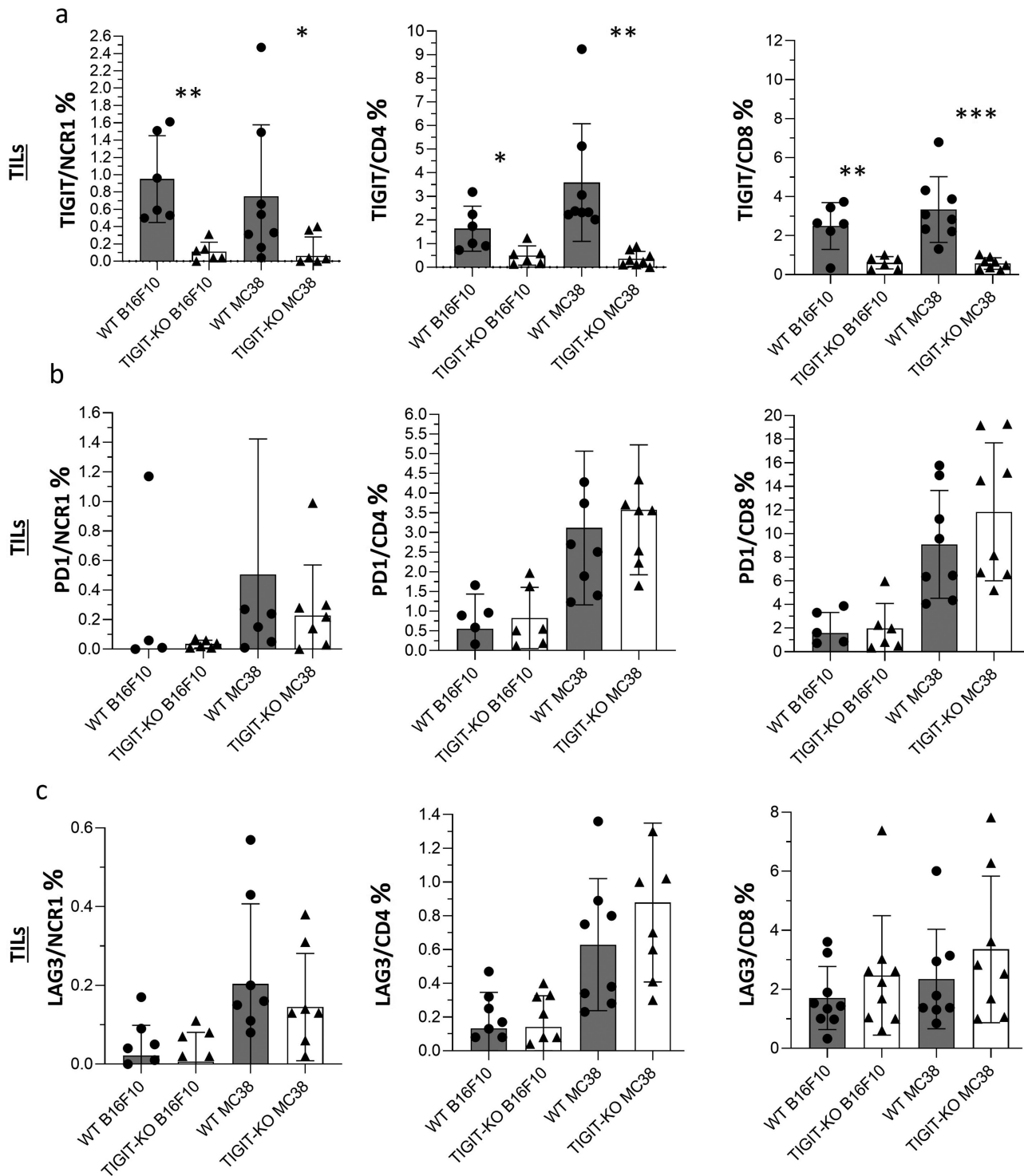
Figure 5. PD-1 and LAG3 are not involved in tumor suppression in Tumor-infiltrating lymphocytes (TILs) of TIGIT KO mice. Bar graphs representing the flow cytometry analysis of isolated TILs obtained from WT and TIGIT KO mice bearing B16F10 and MC38 tumors stained with anti-TIGIT (A) or anti-PD-1 (B) or anti-LAG3 (C) together with anti-mouse Ncr1, anti-mouse CD4, and anti-mouse CD8 antibodies. Values are shown as mean ± SD. *$P < 0.05$, and **$P \le 0.01$, and *** $P \le 0.001$.

reduce B16F10 and MC38 tumor development. Kurtulus et al., for example, found that B16F10 and MC38 tumor growth was delayed in TIGIT knockout mice (TIGIT$^{-/-}$) relative to WT control[28]. Consistently with our results, fewer lung metastases were observed 15 days following i.v. B16F10 tumor challenge in TIGIT$^{-/-}$ compared to the WT mice. Additionally, colon tumor cell-line CT26 was dramatically reduced when treated with the anti-TIGIT blockade antibody and it appears to have

reversed the exhaustion of the TILs[29]. Another study reported that anti-TIGIT therapy alone markedly inhibited B16F10 tumor growth compared with the controls but MC38 inhibition was not significant[30]. These data support our results in that TIGIT deficiency improved anti-tumor response.

Recently, our lab identified the Agglutinin-Like Sequences (ALS) protein family as a novel fungal ligand for TIGIT in both human and mice[10]. *Candida albicans* can also be found in

tumors such as oral[31], colon cancer[32] as well as other forms of cancer[33]. It is currently unknown whether the *Candida*-TIGIT interactions within the tumors will be beneficial in the tumor microenvironment and this issue can be investigated in the future using our TIGIT KO mice. In a pre-clinical study evaluating the correlation between invasive candidiasis (IC), tumors, and inhibitory checkpoint receptors in peripheral blood mononuclear cells (PBMCs), elevated expression of TIGIT and PD-1 on T cells was shown to be increased in patients that died from IC[34].

To date, there are few studies that have examined the association between inflammatory bowel diseases (IBD) and TIGIT. TIGIT expression on IL-17A – producing $CD69^+CD103^-$ $CD4^+$ TRM cells was increased in dextran sodium sulfate (DSS)-induced IBD model in mice, while it was impaired in TIGIT knockout mice. This data suggests that TIGIT knockout protects mice from IBD[35]. Colon carcinogenesis, mucosal ulcerations, and inflammatory cell infiltration caused by dimethylhydrazine (DMH) and/or DSS treatment were reduced in necl-5$^{-/-}$ (PVR-KO) compared to WT mice[36].

In conclusion, we demonstrated that mPVR is the only mTIGIT ligand, using transfectant cells and tumor cell lines. We generated TIGIT knockout mouse model and assessed its functionality *in vitro* in comparison to WT mice. Our findings were further verified *in vivo* using two mouse tumors, B16F10 and MC38, and it was found that TIGIT-KO mice displayed slower tumor growth and reduced tumor weight.

Acknowledgments

Availability of data and materials

The datasets used and/or analyzed during the current study are available from the corresponding author on reasonable request.

Disclosure statement

The authors declare no conflicts of interest.

Funding

References

1. Levi-Schaffer F, Mandelboim O. Inhibitory and coactivating receptors recognising the same ligand: immune homeostasis exploited by pathogens and tumours. Trends Immunol. 2018;39(2):112–122. doi:10.1016/j.it.2017.10.001.

2. Donátová K, Nováková E, Šupolíková M. Immunotherapy for cancer treatment. Klin Onkol. 2022;35(4):284–289. doi:10.48095/ccko2022284.

3. Rotte A. Combination of CTLA-4 and PD-1 blockers for treatment of cancer. J Exp Clin Cancer Res. 2019;38(1):255. doi:10.1186/s13046-019-1259-z.

4. Sasidharan Nair V, Elkord E. Immune checkpoint inhibitors in cancer therapy: a focus on T-regulatory cells. Immunol Cell Biol. 2018;96(1):21–33. doi:10.1111/imcb.1003.

5. Manieri NA, Chiang EY, Grogan JL. TIGIT: a key inhibitor of the cancer immunity cycle. Trends Immunol. 2017;38(1):20–28. doi:10.1016/j.it.2016.10.002.

6. Yu X, Harden K, Gonzalez LC, Francesco M, Chiang E, Irving B, Tom I, Ivelja S, Refino CJ, Clark H, et al. The surface protein TIGIT suppresses T cell activation by promoting the generation of mature immunoregulatory dendritic cells. Nat Immunol. 2009;10(1):48–57. doi:10.1038/ni.1674.

7. Stanietsky N, Rovis TL, Glasner A, Seidel E, Tsukerman P, Yamin R, Enk J, Jonjic S, Mandelboim O. Mouse TIGIT inhibits NK-cell cytotoxicity upon interaction with PVR. Eur J Immunol. 2013;43(8):2138–2150. doi:10.1002/eji.201243072.

8. Jin HS, Park Y. Hitting the complexity of the TIGIT-CD96-CD112R-CD226 axis for next-generation cancer immunotherapy. BMB Rep. 2021;54(1):2–11. doi:10.5483/BMBRep.2021.54.1.229.

9. Gur C, Ibrahim Y, Isaacson B, Yamin R, Abed J, Gamliel M, Enk J, Bar-On Y, Stanietsky-Kaynan N, Coppenhagen-Glazer S, et al. Binding of the Fap2 protein of Fusobacterium nucleatum to human inhibitory receptor TIGIT protects tumors from immune cell attack. Immunity. 2015;42(2):344–355. doi:10.1016/j.immuni.2015.01.010.

10. Charpak-Amikam Y, Lapidus T, Isaacson B, Duev-Cohen A, Levinson T, Elbaz A, Levi-Schaffer F, Osherov N, Bachrach G, Hoyer LL, et al. Candida albicans evades NK cell elimination via binding of Agglutinin-Like Sequence proteins to the checkpoint receptor TIGIT. Nat Commun. 2022;13(1):2463. doi:10.1038/s41467-022-30087-z.

11. Chiang EY, Mellman I. TIGIT-CD226-PVR axis: advancing immune checkpoint blockade for cancer immunotherapy. J ImmunoTher Cancer. 2022;10(4). doi:10.1136/jitc-2022-004711.

12. Cho BC, Abreu DR, Hussein M, Cobo M, Patel AJ, Secen N, Lee KH, Massuti B, Hiret S, Yang JCH, et al. Tiragolumab plus atezolizumab versus placebo plus atezolizumab as a first-line treatment for PD-L1-selected non-small-cell lung cancer (CITYSCAPE): primary and follow-up analyses of a randomised, double-blind, phase 2 study. Lancet Oncol. 2022;23(6):781–792. doi:10.1016/S1470-2045(22)00226-1.

13. Niu J, Maurice-Dror C, Lee DH, Kim DW, Nagrial A, Voskoboynik M, Chung HC, Mileham K, Vaishampayan U, Rasco D, et al. First-in-human phase 1 study of the anti-TIGIT antibody vibostolimab as monotherapy or with pembrolizumab for advanced solid tumors, including non-small-cell lung cancer ☆. Ann Oncol. 2022;33(2):169–180. doi:10.1016/j.annonc.2021.11.002.

14. Mettu NB, Ulahannan SV, Bendell JC, Garrido-Laguna I, Strickler JH, Moore KN, Stagg R, Kapoun AM, Faoro L, Sharma S. A phase 1a/b open-label, dose-escalation study of etigilimab alone or in combination with nivolumab in patients with locally advanced or metastatic solid tumors. Clin Cancer Res. 2022;28(5):882–892. doi:10.1158/1078-0432.CCR-21-2780.

15. Haddad CO, Kalt I, Shovman Y, Xia L, Schlesinger Y, Sarid R, Parnas O. Targeting the Kaposi's sarcoma-associated herpesvirus genome with the CRISPR-Cas9 platform in latently infected cells. Virol J. 2021;18(1). doi:10.1186/s12985-021-01527-x.

16. Reches A, Ophir Y, Stein N, Kol I, Isaacson B, Charpak Amikam Y, Elnekave A, Tsukerman P, Kucan Brlic P, Lenac T, et al. Nectin4 is a novel TIGIT ligand which combines checkpoint inhibition and tumor specificity. J ImmunoTher Cancer. 2020;8(1):e000266. doi:10.1136/jitc-2019-000266.

17. Tomayko MM, Reynolds CP. Determination of subcutaneous tumor size in athymic (nude) mice. Cancer Chemother Pharmacol. 1989;24(3):148–154. doi:10.1007/BF00300234.

18. Stengel KF, Harden-Bowles K, Yu X, Rouge L, Yin J, Comps-Agrar L, Wiesmann C, Bazan JF, Eaton DL, Grogan JL. Structure of TIGIT immunoreceptor bound to poliovirus receptor reveals a cell-cell adhesion and signaling mechanism that requires cis-trans receptor clustering. Proc Natl Acad Sci U S A. 2012;109 (14):5399–5404. doi:10.1073/pnas.1120606109.

19. Liang R, Zhu X, Lan T, Ding D, Zheng Z, Chen T, Huang Y, Liu J, Yang X, Shao J, et al. TIGIT promotes CD8 + T cells exhaustion and predicts poor prognosis of colorectal cancer. Cancer Immunol Immun. 2021;70(10):2781–2793. doi:10.1007/s00262-021-02886-8.

20. Ostroumov D, Duong S, Wingerath J, Woller N, Manns MP, Timrott K, Kleine M, Ramackers W, Roessler S, Nahnsen S, et al. Transcriptome profiling identifies TIGIT as a marker of T-Cell exhaustion in liver cancer. Hepatology. 2020;73(4):2021. doi:10.1002/hep.31466.

21. Kong Y, Zhu L, Schell TD, Zhang J, Claxton DF, Ehmann WC, Rybka WB, George MR, Zeng H, Zheng H. Biology of human tumors T-Cell immunoglobulin and ITIM domain (TIGIT) associates with CD8 þ T-Cell exhaustion and poor clinical outcome in AML patients. Clin Cancer Res. 2016;22(12):3057–3066. doi:10.1158/1078-0432.CCR-15-2626.

22. Chauvin JM, Pagliano O, Fourcade J, Sun Z, Wang H, Sander C, Kirkwood JM, Chen THT, Maurer M, Korman AJ, et al. TIGIT and PD-1 impair tumor antigen–specific CD8+ T cells in melanoma patients. J Clin Invest. 2015;125(5):2046–2058. doi:10.1172/JCI80445.

23. Banta KL, Xu X, Chitre AS, Au-Yeung A, Takahashi C, O'Gorman WE, Wu TD, Mittman S, Cubas R, Comps-Agrar L, et al. Mechanistic convergence of the TIGIT and PD-1 inhibitory pathways necessitates co-blockade to optimize anti-tumor CD8+ T cell responses. Immunity. 2022;55(3):512. doi:10.1016/j.immuni.2022.02.005.

24. Kawashima S, Inozume T, Kawazu M, Ueno T, Nagasaki J, Tanji E, Honobe A, Ohnuma T, Kawamura T, Umeda Y, et al. TIGIT/CD155 axis mediates resistance to immunotherapy in patients with melanoma with the inflamed tumor microenvironment. J ImmunoTher Cancer. 2021;9(11):e003134. doi:10.1136/jitc-2021-003134.

25. Li XY, Das I, Lepletier A, Addala V, Bald T, Stannard K, Barkauskas D, Liu J, Aguilera AR, Takeda K, et al. CD155 loss enhances tumor suppression via combined host and tumor-intrinsic mechanisms. J Clin Invest. 2018;128 (6):2613–2625. doi:10.1172/JCI98769.

26. Iguchi-Manaka A, Kai H, Yamashita Y, Shibata K, Tahara-Hanaoka S, Honda SI, Yasui T, Kikutani H, Shibuya K, Shibuya A. Accelerated tumor growth in mice deficient in DNAM-1 receptor. J Exp Med. 2008;205(13):2959–2964. doi:10.1084/jem.20081611.

27. Han JH, Cai M, Grein J, Perera S, Wang H, Bigler M, Ueda R, Rosahl TW, Pinheiro E, LaFace D, et al. Corrigendum: effective anti-tumor response by TIGIT blockade associated with FcγR engagement and myeloid cell activation. Front Immunol. 2020;11:2445. doi:10.3389/fimmu.2020.615755.

28. Kurtulus S, Sakuishi K, Ngiow SF, Joller N, Tan DJ, Teng MWL, Smyth MJ, Kuchroo VK, Anderson AC. TIGIT predominantly regulates the immune response via regulatory T cells. J Clin Invest. 2015;125(11):4053. doi:10.1172/JCI81187.

29. Zhang Q, Bi J, Zheng X, Chen Y, Wang H, Wu W, Wang Z, Wu Q, Peng H, Wei H, et al. Blockade of the checkpoint receptor TIGIT prevents NK cell exhaustion and elicits potent anti-tumor immunity. Nat Immunol. 2018;19(7):723–732. doi:10.1038/s41590-018-0132-0. 2018 19:7.

30. Zhao K, Jiang L, Si Y, Zhou S, Huang Z, Meng X. TIGIT blockade enhances tumor response to radiotherapy via a CD103 + dendritic cell-dependent mechanism. Cancer Immunol Immunother. 2023;72(1):193–209. doi:10.1007/s00262-022-03227-z.

31. Sultan AS, Theofilou VI, Alfaifi A, Montelongo-Jauregui D, Jabra-Rizk MA. Is Candida albicans an opportunistic oncogenic pathogen? PLoS Pathog. 2022;18(4):e1010413. https://doi.org/10.1371/journal.ppat.1010413

32. Conche C, Greten FR. Fungi enter the stage of colon carcinogenesis. Immunity. 2018;49(3):384–386. doi:10.1016/j.immuni.2018.09.002.

33. Chung LM, Liang JA, Lin CL, Sun LM, Kao CH. Cancer risk in patients with candidiasis: a nationwide population-based cohort study. Oncotarget. 2017;8(38):63562–63573. doi:10.18632/oncotarget.18855.

34. Mellinghoff SC, Thelen M, Bruns C, Garcia-Marquez M, Hartmann P, Lammertz T, Lehmann J, Nowag A, Stemler J, Wennhold K, et al. T-cells of invasive candidiasis patients show patterns of T-cell-exhaustion suggesting checkpoint blockade as treatment option. J Infect. 2022;84(2):237–247. doi:10.1016/j.jinf.2021.12.009.

35. Chen B, Ye B, Li M, Wang S, Li J, Lai Y, Yang N, Ke Z, Zhang H. TIGIT deficiency protects mice from DSS-Induced colitis by regulating IL-17A-producing CD4 + Tissue-Resident memory T cells. Front Immunol. 2022;13. doi:10.3389/fimmu.2022.931761.

36. Abe A, Fukui H, Fujii S, Kono T, Mukawa K, Yoshitake N, Sekikawa A, Ichikawa K, Tomita S, Yamagishi H, et al. Role of Necl-5 in the pathophysiology of colorectal lesions induced by dimethylhydrazine and/or dextran sodium sulphate. J Pathol. 2009;217(1):42–53. doi:10.1002/path.2431.